

The influence of galactic cosmic rays on ion–neutral hydrocarbon chemistry in the upper atmospheres of free-floating exoplanets

P. B. Rimmer¹, Ch. Helling¹ and C. Bilger²

¹*SUPA, School of Physics and Astronomy, University of St Andrews, St Andrews KY16 9SS, UK e-mail: pr33@st-andrews.ac.uk*

²*Department of Engineering, University of Cambridge, Cambridge CB2 1PZ, UK*

Abstract: Cosmic rays may be linked to the formation of volatiles necessary for prebiotic chemistry. We explore the effect of cosmic rays in a hydrogen-dominated atmosphere, as a proof-of-concept that ion–neutral chemistry may be important for modelling hydrogen-dominated atmospheres. In order to accomplish this, we utilize Monte Carlo cosmic ray transport models with particle energies of $10^6 \text{ eV} < E < 10^{12} \text{ eV}$ in order to investigate the cosmic-ray enhancement of free electrons in substellar atmospheres. Ion–neutral chemistry is then applied to a DRIFT–PHOENIX model of a free-floating giant gas planet. Our results suggest that the activation of ion–neutral chemistry in the upper atmosphere significantly enhances formation rates for various species, and we find that C_2H_2 , C_2H_4 , NH_3 , C_6H_6 and possibly C_{10}H are enhanced in the upper atmospheres because of cosmic rays. Our results suggest a potential connection between cosmic-ray chemistry and the hazes observed in the upper atmospheres of various extrasolar planets. Chemi-ionization reactions are briefly discussed, as they may enhance the degree of ionization in the cloud layer.

Received 29 July 2013, accepted 4 December 2013

Key words: astrochemistry, atmospheres, atmospheric effects, cosmic rays, planets and satellites.

Introduction

Life requires a considerable variety of chemical ingredients, and these ingredients are composed mostly of four elements: hydrogen, carbon, nitrogen and oxygen. The backbone species for prebiotic chemistry include the reactive species HCHO, HCN, ethylene, cyanoacetylene and acetylene (Miller & Cleaves 2006), and it is an open question how or even where these species were first formed, whether in the interstellar medium (Hoyle & Wickramasinghe 2000), on the backs of meteorites, in the atmosphere or deep within the oceans of the archaic earth (Orgel 1998). Energetic processes, such as photolysis and cosmic-ray ionization affect atmospheric and geological chemistry on Earth, and may have an important role to play in the formation of prebiotically relevant radical species. The atmosphere of Jupiter and Jupiter-like planets provide a natural laboratory in which to study the effects energetic processes have on hydrocarbon and organic chemistry. The atmospheres of giant gas planets are hydrogen dominated and have significant elemental concentrations of carbon and oxygen (Lodders 2004), and many of the same energetic processes take place in their atmospheres as on Earth, such as photodissociation (Moses *et al.* 2005), cosmic-ray ionization (Whitten *et al.* 2008) and lightning (Gurnett *et al.* 1979).

There has been significant work on cosmic-ray transport and ionization in the atmosphere of Titan. The effect cosmic rays

have on ionizing and dissociating carbon and nitrogen species (Capone *et al.* 1980, 1983; Molina-Cuberos *et al.* 1999a), enhancing the formation of aerosols (Sittler *et al.* 2010), and the role of cosmic rays in instigating lightning (Borucki *et al.* 1987) have been explored. Cosmic-ray transport in Titan has also been investigated (for example, Molina-Cuberos *et al.* 1999b). In terms of electron production, the transport model for Titan bears qualitatively similar results to the cosmic-ray transport models on Earth (e.g., Velinov *et al.* 2009). If results are cast in terms of column density, both seem to be well-fit by a Poisson distribution and peak at roughly the same atmospheric depth ($\sim 100 \text{ g cm}^{-2}$). Initial studies on cosmic-ray ionization in Jupiter (Whitten *et al.* 2008) and exoplanets (Rimmer & Helling 2013) support this result.

The effects of cosmic-ray ionization on the chemistry of extrasolar planet atmospheres have not yet been investigated, although Moses *et al.* (2011) speculate that cosmic-ray ionization may be connected to the hazes in the upper atmosphere of HD 189733b observed by Pont *et al.* (2008) and Sing *et al.* (2011). An investigation into hydrocarbon chemistry in the atmospheres of extrasolar giant gas planets is interesting from an astrobiological perspective because such a study will provide insight into the significance of different initial conditions and physical parameters on this prebiotic chemistry. We present a proof-of-concept on the potential effect of cosmic rays in the atmosphere between $10 \mu\text{bar}$ and

1 nbar. In order to accomplish this we take the results of cosmic-ray ionization on a DRIFT-PHOENIX model atmosphere of a Jupiter-like planet from Rimmer & Helling (2013), and apply them to an astrochemical network adapted to the atmospheric environment of a Jupiter-like planet. A brief description of DRIFT-PHOENIX and the cosmic-ray transport is provided in ‘The model atmosphere and cosmic-ray transport’ section. We then discuss the chemical network and its results in ‘Gas-phase chemical kinetics model’ section.

The model atmosphere and cosmic ray transport

The chemical calculations in the following section are built upon a model atmosphere of DRIFT-PHOENIX (from Dehn 2007; Helling *et al.* 2008; Witte *et al.* 2009), and cosmic-ray transport calculations from Rimmer & Helling (2013). DRIFT-PHOENIX is a model that self-consistently combines the calculation of hydrostatic equilibrium and comprehensive radiative transfer for a substellar object or warm exoplanet with a dust formation model that incorporates seed nucleation, growth, gravitational settling and evaporation of dust grains. This self-consistent approach has the advantage of capturing the effect of the dust on the gas-phase, e.g., the elemental depletion and the backwarming effect of the dust on the gas-phase temperature. DRIFT-PHOENIX has been utilized in explorations of non-thermodynamic charging of the atmosphere by, e.g., dust–dust collisions and Alfvén ionization (Helling *et al.* 2011; Stark *et al.* 2013). This model takes as input elemental abundances, effective temperature (T_{eff} , K) and surface gravity ($\log g$, with g in units of cm s^{-2}). The example atmosphere we consider here is that of a model free-floating exoplanet, with $\log g = 3$, $T_{\text{eff}} = 1000$ K and solar metallicity. The pressure–temperature structure of the model is plotted in Fig. 1.

We apply a Monte Carlo model to determine cosmic-ray transport for cosmic rays of energy $E < 10^9$ eV. In this model, detailed in Rimmer *et al.* (2012), we take 10 000 cosmic rays and propagate them through a model exosphere (Rimmer & Helling 2013, their Section 2) and DRIFT-PHOENIX atmosphere. The cosmic rays travel a distance such that $\sigma \Delta N = 1$ (σ [cm^2] denotes the collisional cross-section between the cosmic ray and a gas-phase atmospheric species, and ΔN [cm^{-2}] is the column density of the distance travelled). A fraction of the cosmic rays will have experienced a collision and will lose some of their energy, $W(E)$ [eV]. Alfvén wave generation by cosmic rays is also accounted for (Skilling & Strong 1976).

An analytical form for the column-dependent ionization rate, Q , as a function of column density, N_{col} [cm^{-2}] from Rimmer & Helling (2013) is:

$$Q(N_{\text{col}}) = Q_{\text{HECR}}(N_{\text{col}}) + \zeta_0 n_{\text{gas}} \times \begin{cases} 480 & \text{if } N_{\text{col}} < N_1 \\ 1 + (N_0/N_{\text{col}})^{1.2} & \text{if } N_1 < N_{\text{col}} < N_2 \\ e^{-kN_{\text{col}}} & \text{if } N_{\text{col}} > N_2 \end{cases} \quad (1)$$

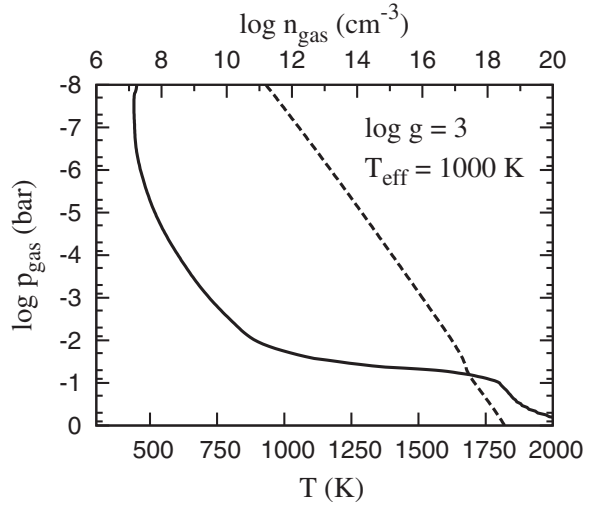


Fig. 1. The temperature, T [K] (solid, bottom) and density, $\log n_{\text{gas}}$ [cm^{-3}] (dashed, top) plotted as a function of pressure, $\log p_{\text{gas}}$ [bar], for our model DRIFT-PHOENIX atmosphere, when $\log g = 3$, $T_{\text{eff}} = 1000$ K, and at solar metallicity.

where $\zeta_0 = 10^{-17} \text{ s}^{-1}$ is the standard ionization rate in the dense interstellar medium, and the column densities $N_0 = 7.85 \times 10^{21} \text{ cm}^{-2}$, $N_1 = 4.6 \times 10^{19} \text{ cm}^{-2}$, $N_2 = 5.0 \times 10^{23} \text{ cm}^{-2}$ and $k = 1.7 \times 10^{-26} \text{ cm}^2$ are fitting parameters. The value for the high-energy cosmic-ray ionization rate, $Q_{\text{HECR}}(N_{\text{col}})$ is given in Rimmer & Helling (2013, their Fig. 5).

For cosmic rays with $E > 10^9$ eV, the cosmic-ray transport is treated by the analytical form of Velinov & Mateev (2008); Velinov *et al.* (2009), appropriately modified for our model atmosphere. Rimmer & Helling (2013) provide a detailed description of the modifications to the calculations of Velinov & Mateev (2008) and Rimmer *et al.* (2012).

Gas-phase chemical kinetics model

Now that the rate of electron production by galactic cosmic rays is determined, we study the effect that this rate will have on the atmospheric gas by applying a gas-phase network. Our chemical model allows us to explore first findings with respect to the local hydrocarbon chemistry. The electrons in the atmosphere will be freed by cosmic rays and by the secondary photons produced from their interaction with the gas. Secondary photons are generated via the Prasad–Tarafdar mechanism (Prasad & Tarafdar 1983). We utilize the detailed emission spectrum from Gredel *et al.* (1989). Photoionization and photodissociation rates for secondary photons are included in the model. The rate of collisional de-excitation varies throughout the atmosphere. At the upper limit for our model, $T_{\text{gas}} = 800$ K, the H_2 number density is $\sim 10^{14} \text{ cm}^{-3}$ for our model giant gas planet atmosphere. The cross-section for collisional de-excitation is of the order of $\sigma_{\text{coll}} \sim 10^{-23} - 10^{-22} \text{ cm}^2$ (Shull & Hollenbach 1978), corresponding to a timescale for collisional de-excitation of $t_{\text{coll}} \approx (n_{\text{gas}} \sigma_{\text{coll}} v_{\text{coll}})^{-1} \sim 100$ s, where v_{coll} is the average collisional velocity of the gas at 800 K. This is much longer than the timescale for spontaneous emission (Prasad &

Tarafdar 1983), and so we ignore the effect of collisional de-excitation on our emission spectrum. Millar *et al.* (1997); McElroy *et al.* (2013) claim that the photoionization and photodissociation rates for secondary photons are valid over a temperature range of $10 \text{ K} < T_{\text{eff}} < 41\,000 \text{ K}$.

Free electrons will also be destroyed by recombination processes, e.g., with ions. We compare these two competing processes in detail: if the cosmic-ray ionization rate is much greater than the recombination rate, then we can expect a significant electron enhancement from cosmic rays. If, however, the recombination is much more rapid than the ionization, then the number of free electrons will remain low. We examine these two rates by concentrating on the number of free electrons produced by cosmic rays and cosmic-ray photons. We utilize a self-consistent gas-phase time-dependent chemical model that includes various cosmic ray, secondary electron and secondary photo-ionization chemical processes, and recombination reactions (described below). This model is calculated iteratively at different depths with the value of Q [$\text{cm}^{-3} \text{ s}^{-1}$] calculated using Rimmer & Helling (2013, their equation 23). As result of this procedure, we determine the number of free electrons and chemical abundances as a function of the local atmospheric pressure for our model giant gas planet atmosphere.

The kinetic gas-phase chemistry model

Various chemical kinetics networks have been developed to model the non-equilibrium atmospheric chemistry of giant gas planets (Moses *et al.* 2000; Zahnle *et al.* 2009; Venot *et al.* 2012). Bilger *et al.* (2013) introduce a new approach to non-equilibrium chemistry that explores individual and immediate destruction reactions for various species absent from the gas-phase in the upper atmosphere. These models involve robust chemical networks and calculate radiative transfer and vertical mixing, but they do not account for ion–neutral chemistry. We thus have adapted an interstellar chemical model with a detailed cosmic-ray chemistry in order to calculate the impact of cosmic rays on the degree of ionization by chemical kinetic processes. Molecular hydrogen dominates throughout our model atmospheres, and interstellar kinetics models contain a detailed treatment of the cosmic-ray ionization of H and H_2 , among other species, as well as recombination rates for all ions included in the networks.

The density profile and equilibrium chemical abundances for the atmosphere, from the exobase and through the cloud layer, are taken from the DRIFT–PHOENIX model atmosphere results. The chemical kinetics are modelled using the NAHOON gas-phase time-dependent astrochemical model (Wakelam *et al.* 2005, 2012). The newest version of this code can model objects with temperatures of $T \lesssim 800 \text{ K}$ (Harada *et al.* 2010). We use the high-temperature OSU 2010 Network from http://physics.ohio-state.edu/~eric/research_files/osu_09_2010_ht.

This network comprises 461 species and well over 4000 reactions, including cosmic-ray ionization, photo-ionization, photo-dissociation, ion–neutral and neutral–neutral reactions. The additional reactions from the high-temperature network of Harada *et al.* (2010) include processes with activation energies

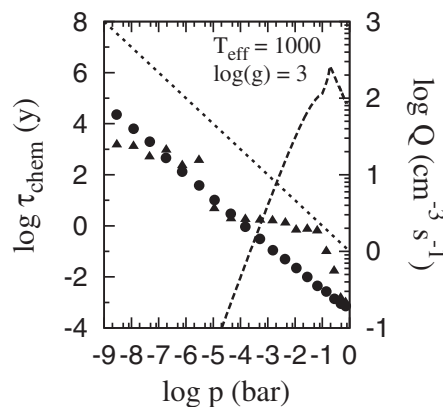


Fig. 2. The chemical relaxation timescale towards steady state, τ_{chem} , as a function of the local gas pressure, for the giant gas planet model atmosphere ($T_{\text{eff}} = 1500$, $\log g = 3$, solar metallicity). Each data point represents the time for the NAHOON model to achieve steady state, with cosmic rays (triangles, left axis) and without cosmic rays (circles, left axis). The dotted line (left axis) represents the total runtime for the NAHOON model. The divergence from $1/n_{\text{gas}}$ in runtimes is probably due to the higher number of free electrons produced by cosmic rays. The cosmic ray electron production rate, Q [$\text{cm}^{-3} \text{ s}^{-1}$], is also shown (dashed line, right axis).

of magnitude $\sim 2000 \text{ K}$, reverse reactions and collisional dissociation.

We effectively apply a model at our model atmosphere for the chemical composition at different atmospheric heights. For irradiated atmospheres and atmospheres of rotating bodies, vertical mixing can be significant, especially in the upper atmosphere. For non-rotating planets far from their host star, however, vertical mixing timescales are of the order of $10^3 - 10^7$ years (Woitke & Helling 2004, esp. their Fig. 2), and are orders of magnitude longer than the chemical timescales over the entire range of atmospheric pressures. We therefore expect that the atmospheric chemistry can effectively be treated as a series of zero-dimensional chemical networks. For irradiated atmospheres, vertical mixing timescales can be much shorter (Showman *et al.* 2009; Moses *et al.* 2011). For initial abundances at each height, we use the thermodynamic equilibrium abundances calculated in the manner described by Bilger *et al.* (2013), where available. If the thermochemistry is not calculated for a given species in the OSU high Temperature network, we set the initial abundances equal to zero. The model is calculated until it reaches steady-state. We have not yet explored the effect of varying the initial abundances.

Because our model is applied to a hypothetical free-floating giant gas planet, vertical mixing and UV photoionization need not be accounted to approximate the non-equilibrium chemistry, because these processes are expected to be negligible in such an environment. This is appropriate for a first proof-of-concept, but it does mean that our methods cannot be directly applied to irradiated planets, where vertical mixing timescales are short and UV photoionization and photodissociation has a major effect on chemistry in the upper atmosphere. We plan to apply an expanded version of our ion–neutral network to a Hot Jupiter in a future paper.

Our model does not account for termolecular neutral–neutral or ion–neutral reactions. At some atmospheric density, termolecular reactions will become important. In order to estimate when this is, we follow the example of Aikawa *et al.* (1999) and calculate the ‘typical’ rate for a bimolecular reaction ($k_2 \sim 10^{-11} \text{ cm}^6 \text{ s}^{-1}$) divided by a ‘typical’ rate for a termolecular reaction, ($k_3 \sim 10^{-30} \text{ cm}^6 \text{ s}^{-1}$):

$$\frac{k_2}{k_3} \sim 10^{19} \text{ cm}^{-3} \quad (2)$$

Our critical density below which three-body neutral–neutral reactions are not significant would be $n_c \sim 10^{17} \text{ cm}^{-3}$. Alternatively, Woods & Willacy (2007) estimate that $n_c \sim 10^{14} \text{ cm}^{-3}$. If we use the lower value, then the critical pressure, above which termolecular reactions dominate, is $p_c \approx 10^{-5} \text{ bar}$. If we use the higher value of $\sim 10^{17} \text{ cm}^{-3}$, then the cutoff moves to higher pressure, of about $p_c \approx 0.1 \text{ bar}$. We use the stronger limit of $n_c \sim 10^{14} \text{ cm}^{-3}$.

NAHOON treats the kinetic chemistry as a series of rate equations. A given rate equation for a species A formed by $B + C \rightarrow A + X$, and destroyed by $A + D \rightarrow Y + Z$, is of the form:

$$f_1 = \frac{dn(A)}{dt} = k_{BC}n(B)n(C) - k_{AD}n(A)n(D) + \dots \quad (3)$$

where k_{BC}, k_{AD} are the rates of formation and destruction of A , respectively. We can represent the rate equation for the i -th species as f_i , i ranging from 1 to the total number of species, N . This system of equations has the Jacobian:

$$J = \begin{pmatrix} \partial f_1 / \partial n_1 & \dots & \partial f_1 / \partial n_N \\ \vdots & \ddots & \vdots \\ \partial f_N / \partial n_1 & \dots & \partial f_N / \partial n_N \end{pmatrix} \quad (4)$$

where N is the total number of gas-phase species.

We run this model for the whole temperature–density profile for the model atmosphere considered here. We allow the network to evolve to steady state, and the time the system takes to reach steady state depends on the atmospheric depth. The timesteps decrease in proportion to the increasing total density. The relaxation timescale for the model can be determined from the inverse of the Jacobian of the system taken when all the species in the system have reached a steady state: $n_i = \overset{\circ}{n}_i$ for a given species, i , and $f_i \equiv f(\overset{\circ}{n}_i) = 0$. Specifically, one can determine the relaxation timescale, τ_{chem} , to achieve steady state to be equal to the inverse of the eigenvalue, λ_i , with the smallest absolute real component, or Woitke *et al.* (2009, their Eq. 117):

$$\tau_{\text{chem}} = \max|\text{Re}\{\lambda_i\}^{-1}| \quad (5)$$

For the eigen-vectors of the Jacobian, j :

$$Jj = \lambda_j j \quad (6)$$

All λ_i must have the same proportionality relationship as the components of J , so:

$$\lambda_i \propto \frac{\partial f_i}{\partial n_i} \propto \frac{f_i - \overset{\circ}{f}_i}{n_i - \overset{\circ}{n}_i} \quad (7)$$

Since the deviation from steady state, $n_i - \overset{\circ}{n}_i$, is proportional to the total density of the system, $n_{\text{gas}} = \sum n_i$, and the deviation $f_i - \overset{\circ}{f}_i = f_i$ is proportional to n_{gas}^2 for two-body reactions, it follows that:

$$\tau_{\text{chem}} \propto \frac{1}{n_{\text{gas}}} \quad (8)$$

We run NAHOON until steady state, $\overset{\circ}{t} = \tau_{\text{chem}}$, with timesteps proportional to τ_{chem} and therefore to $1/n_{\text{gas}}$. Equation (8) does not account for the temperature dependence. Also, first-order reactions, particularly the cosmic-ray ionization reactions, will have relaxation times that scale differently with n_{gas} and this is why the time to equilibrium is different with cosmic-ray ionization than without cosmic-ray ionization. Ionization rate coefficients for certain species are quite small, and this can increase the time to steady-state. A complete determination of τ_{chem} therefore would require solving equation (5). In practice, however, we find that adjusting the runtime of NAHOON by the proportionality $1/n_{\text{gas}}$ achieves steady state at each point in the atmosphere. Figure 2 contains a plot of τ_{chem} as a function of the atmospheric gas pressure both with and without cosmic-ray ionization. The figure shows that significantly different amounts of time are required in order to reach steady state for different depths. Near the exobase, the timescale can be of the order of 10^3 years, whereas in the cloud layer τ_{chem} is of the order of hours. When cosmic-ray ionization is included, τ_{chem} is less than $1/n_{\text{gas}}$ by two orders of magnitude in the very upper atmosphere, and is greater than $1/n_{\text{gas}}$ by more than an order of magnitude within the cloud layer. At the cloud base, however, the value of τ_{chem} with cosmic rays converges to the value of τ_{chem} without cosmic rays.

Cosmic-ray ionization is included in the OSU network as rates with coefficients, α_X , scaling the primary ionization rate for the reaction X such that $\zeta_X = \alpha_X \zeta_p$. The NAHOON model is iterated towards steady state at different depths, where the local gas density and temperature ($n(z)$, $T(z)$) and the cosmic-ray flux density change with depth. External UV fields are not considered in this study, in order to clearly identify the cosmic-ray contribution to ionization. The impact of photons generated by the secondary electrons, so-called cosmic-ray photons, is included, however.

The results of our network provide some interesting predictions for free-floating giant gas planets. Some of these results may be applicable also to irradiated exoplanets, although the enhanced mixing and photochemistry may drastically change some of these predictions. First, our results predict where the free charges, both positive and negative, are likely to reside, chemically. Our model predictions for the most abundant cations and anions are presented in subsection ‘Atmospheric cations and anions’. Because the focus of this paper is on prebiotic chemistry, and because of the strong effect cosmic rays have upon them, complex hydrocarbons are the neutral species of most interest. Our results for complex hydrocarbons are presented in subsection ‘Cosmic rays and carbon chemistry in the upper atmosphere’. In this section, we also discuss a neutral–neutral reaction that produces free

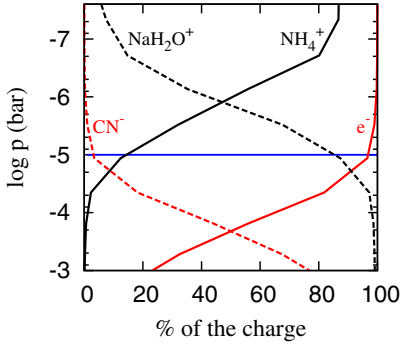


Fig. 3. The percentage of positive (black) and negative (red) charge contained by a given species as a function of pressure, p [bar] for our model giant gas planet atmosphere ($T_{\text{eff}}=1000$ K, $\log g=3$). The negative charge is mostly in the form of electrons and CN^- . The positive charge is carried primarily by NH_4^+ in the upper atmosphere and NaH_2O^+ in the cloud layer. The rest of the positive charge is mostly in the form of large carbon-containing ions, e.g., C_7H_2^+ , C_7H_3^+ and C_8H_4^+ . A blue horizontal line indicates the pressure above which termolecular reactions may dominate.

electrons, and will speculate on its effect on the degree of ionization within a brown dwarf atmosphere. Subsection ‘Ammonia’ concludes our discussion on chemistry.

Atmospheric cations and anions

According to our chemical network, cosmic rays primarily ionize H_2 , H_2O , C and He, the most abundant neutral species in the upper atmosphere of an oxygen-rich, hydrogen-dominated planet. The ions H_2^+ , H_2O^+ , C^+ and He^+ do not retain the bulk of the excess positive charge for long, but react away or exchange their excess charge.

We find that for our model exoplanet atmosphere, when $p_{\text{gas}} < 10^{-6}$ bar, up to 90% of positive charge is carried by NH_4^+ , and the rest of the positive charge is carried by various large carbon-bearing cations. When $p_{\text{gas}} > 10^{-6}$ bar, the most abundant cation becomes NaH_2O^+ , carrying more than 95% of the charge for $p_{\text{gas}} > 5 \times 10^{-4}$ bar. There are two reasons for the transition between these two species: cosmic-ray ionization and enhanced charge exchange at high densities. Figure 3 shows which species carry most of the positive charge.

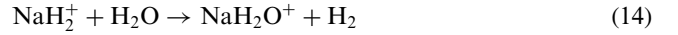
In the upper atmosphere, NH_4^+ is formed primarily by the reactions:



Reactions (9)–(11) are also the dominant formation pathways for the cyanopolynes in the upper atmosphere. The large cations $\text{C}_{2n+1}\text{H}_2\text{N}^+$ as well as H_3O^+ are connected, via H_3^+ , to cosmic-ray driven chemistry. Since the cosmic rays do not penetrate through the cloud layer, the $\text{C}_{2n+1}\text{H}_2\text{N}^+$ ions become depleted, and NH_4^+ is no longer efficiently formed.

At $p_{\text{gas}} > 10^{-6}$ bar, as the gas density increases, collisions become more frequent and charge exchange reactions

dominate. Atomic sodium collects a large amount of the charge through these charge exchange reactions. Then:



which proceed rapidly because of the high abundances of H_2 and water. NH_4^+ and NaH_2O^+ are both destroyed mostly by dissociative recombination.

Cosmic rays and carbon chemistry in the upper atmosphere

It has been suggested that cosmic rays enhance aerosol production in the terrestrial atmosphere (e.g., Shumilov *et al.* 1996) and that they potentially initiate chemical reactions that allow the formation of mesospheric haze layers such as those observed on the exoplanet HD 189733b by Pont *et al.* (2008) and Sing *et al.* (2011) and those observed on Titan (Rages & Pollack 1983; Porco *et al.* 2005; Liang *et al.* 2007; Lavvas *et al.* 2009). We are interested in the effects that cosmic rays can have on the carbon chemistry in extraterrestrial, oxygen-rich atmospheres, such as those of giant gas planets. Especially relevant are the chemical abundances of the largest carbon species in the gas-phase model, which is likely connected to Polycyclic Aromatic Hydrocarbon (PAH) production in planetary atmospheres (Wilson & Atreya 2003). Although our network does not incorporate a complete PAH chemistry, it does contain chemical pathways that reach into long carbon chains, the longest chain being C_{10}H .

The most meaningful information from our chemical model is the enhanced or reduced abundance of various species due to ion–neutral chemistry, compared with their abundances according to purely neutral–neutral chemistry. Although this shows us the effect cosmic-ray driven chemistry can have on the abundances of carbon bearing species, it does not tell us whether these enhancements are observable. An enhancement of ten orders of magnitude on a species with a volume fraction, from 10^{-40} to 10^{-30} , is significant, but unobservable. In order to answer this question, we apply the thermochemical equilibrium results for a $\log g = 3$, 1000 K atmosphere using the calculations from Bilger *et al.* (2013), to the degree that the various species have been enhanced or reduced. We take the chemical equilibrium number density of a species, X , $n_{\text{eq}}(X)$ [cm^{-3}] and solve for the non-equilibrium abundance, $n_{\text{neq}}(X)$ [cm^{-3}] by:

$$n_{\text{neq}}(X) = \zeta n_{\text{eq}}(X) \quad (16)$$

where ζ is the amount that the abundance is enhanced or reduced by cosmic rays. We plot the predicted volume fractions of CO , CO_2 , H_2O , CH_4 , C_2H_2 , C_2H_4 and NH_3 , as a function of pressure, in Fig. 4. Although C_2H and C_{10}H are also enhanced by orders of magnitude, the results are not shown in this figure. For C_2H , this is because the resulting volume fraction is lower than 10^{-20} throughout the model atmosphere. For C_{10}H , this is because the equilibrium concentration is unknown. The results for cosmic-ray enhancement are not reliable when $p_{\text{gas}} > 10^{-5}$ bar because termolecular reactions may begin to take over. When this happens, so long as vertical mixing timescales

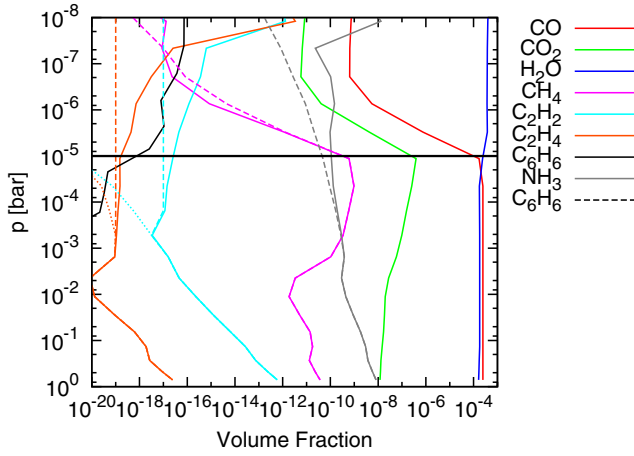


Fig. 4. Volume fraction of various species as a function of the gas pressure, p [bar] for the model atmosphere of a free-floating giant gas planet ($T_{\text{eff}} = 1000$ K, $\log g = 3$), obtained by combining our results to those of Bilger *et al.* (2013). The results of Bilger *et al.* (2013, dotted), the results assuming chemical quenching of C_2H_2 and C_2H_4 at height at $\sim 10^{-3}$ (dashed), and the results with cosmic ray ionization (solid) are all presented in this plot. A thick black horizontal line indicates the pressure above which termolecular reactions may dominate.

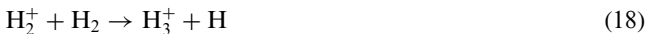
are not too small, the added reactions will bring the system to thermochemical equilibrium; equilibrium abundances are also presented in the figure.

C_2H_2 and C_2H_4

For the predicted cosmic-ray enhancement of C_2H_2 and C_2H_4 , we assume chemical quenching at 10^{-3} bar, although it may well be quenched at much higher pressures of ~ 0.01 bar (Moses *et al.* 2011). With this assumption, we find that both C_2H_2 and C_2H_4 are brought to volume fractions of $\sim 10^{-12}$ when $p_{\text{gas}} \approx 10^{-8}$ bar. This is compared to the quenched abundance in the absence of cosmic rays, of $\sim 10^{-17}$ for C_2H_2 and $\sim 10^{-19}$ for C_2H_4 .

Carbon monoxide and methane are largely unaffected by cosmic-ray ionization, although methane is depleted by about one order of magnitude at 10^{-8} bar. Both methane and carbon monoxide decrease rapidly with decreasing pressure when $p_{\text{gas}} \lesssim 10^{-6}$ bar and, according to Bilger *et al.* (2013), at these pressures and temperatures a significant amount of the carbon is atomic. The cosmic-ray chemistry does impact methane, but only in the very upper atmosphere, where it is not very abundant. Cosmic rays deplete the methane by approximately one order of magnitude, from a volume fraction of 10^{-16} – 10^{-17} .

Acetylene and ethylene, as well as C_2H , are enhanced by various complex reaction pathways. One such pathway to acetylene, dominant at 10^{-8} bar, when there is a high fraction neutral carbon, is:



There are dozens of pathways from H_3^+ to the complex hydrocarbons listed above, and it would be beyond the scope of this paper to list which multiple pathways dominate at different atmospheric heights. Nevertheless, the above reaction pathway gives some insight into the manner in which ion–neutral chemistry can enhance complex hydrocarbons at the cost of other carbon-bearing species, such as methane. Acetylene and ethylene may have an interesting connection to hazes observed in some exoplanets; they are specifically mentioned by Zahnle *et al.* (2009) as possibly contributing to the hazes observed in HD 189733b and other exoplanets (Pont *et al.* 2008; Bean *et al.* 2010; Demory *et al.* 2011; Sing *et al.* 2011).

Although our model is not directly applicable to irradiated exoplanets, we can speculate what would happen on such planets, by examining the results of comprehensive photochemical models. Moses *et al.* (2011), for example, indicate that UV photochemistry is efficient at destroying the C_2H_2 in HD189733b when $p_{\text{gas}} \lesssim 10 \mu\text{bar}$ (see their Fig. 3). They do find far higher abundances for C_2H_2 overall, such that its volume fraction at 10^{-8} with photodissociation and mixing but without cosmic rays may be $\sim 10^{-20}$. If so, the cosmic-ray enhanced volume fraction may approach 10^{-11} at $p_{\text{gas}} = 10^{-8}$ bar. Confirming these speculative results will require a comprehensive photochemistry self-consistently combined with the cosmic-ray chemistry.

Long polyacetylene radicals are believed to contribute to PAH and other soot formation both in the interstellar medium (Frenklach & Feigelson 1989) and in atmospheres of e.g., Titan (Wilson & Atreya 2003). In an atmospheric environment, polyacetylene radicals tend to react with polyacetylenes to produce longer chains (Wilson & Atreya 2003, their R1, R2). Further chains can build upon radical sites on these polyacetylenes and may lead to cyclization of the structure, possibly initiating soot nucleation (Krestinin 2000). Although our network does not incorporate near this level of complexity, our model does include the constituent parts of this process: C_2H_2 and C_nH . These species currently seem to be the most likely candidate constituents for PAH growth.

C_{10}H and C_6H_6

According to our calculations, one of the most common ions to experience dissociative recombination in the upper atmosphere is $\text{C}_{10}\text{H}_2^+$. The favoured dissociative recombination of this large carbon-chain cation in our network is:



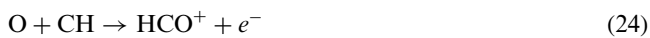
The cosmic-ray ionization results in an exceptionally high steady-state fractional abundance of C_{10}H in the very upper atmosphere of exoplanet ($p_{\text{gas}} \sim 10^{-6}$), corresponding to a density of $n(\text{C}_{10}\text{H}) \approx 1000 \text{ cm}^{-3}$, or a fractional abundance of $n(\text{C}_{10}\text{H})/n_{\text{gas}} \sim 10^{-10}$. It is unlikely that a long polyacetylene radical would be so abundant in exoplanetary atmospheres because of the numerous destruction pathways that should

exist in a high-temperature high-density environment for a species so far from thermochemical equilibrium. Planetary atmospheres are expected to favour aromatic over aliphatic species, and partly for this reason, the high abundance predicted by our model nevertheless suggests possibly enhanced abundances of larger hydrocarbons built up from reactions between $C_{10}H$ and C_2H_2 .

Our model also includes the simple mono-cyclic aromatic hydrocarbon benzene. We find that cosmic rays enhance the abundance of benzene in the upper atmosphere, when $p_{\text{gas}} \lesssim 10^{-6}$ bar, by several orders of magnitude. Since benzene normally has a very small volume fraction ($< 10^{-50}$) at these low pressures, we assume a quenching scale height of $p_{\text{gas}} = 10^{-3}$ bar, and find that the volume fraction of benzene still remains well below 10^{-20} in the absence of cosmic rays, but does achieve a volume fraction of $\sim 10^{-16}$ when cosmic rays are present. Although this is a significant enhancement, benzene would be very difficult to observe at this volume fraction.

Chemi-ionization

The OSU chemical network used in the NAHOON code also provides us with an opportunity to explore purely chemical avenues for enhancing ionization. The single reaction involving two neutral species that impacts the ionization is the chemi-ionization reaction:



This reaction has a rate coefficient of $k = 2 \times 10^{-11} (T/300 \text{ K})^{0.44} \text{ cm}^3 \text{ s}^{-1}$, accurate to within 50% at $T < 1750 \text{ K}$ (MacGregor & Berry 1973). We can use the energetics from MacGregor & Berry (1973) to construct the reverse reaction, following the method of Visscher & Moses (2011). The reverse reaction is slightly endothermic, with an activation energy of $\sim 0.4 \text{ eV}$, or $\Delta E \approx 4600 \text{ K}$. These reaction taken together will consistently produce a steady-state degree of ionization, $f_e = n(e^-)/n_{\text{gas}} \sim 10^{-11}$ in our model. This degree of ionization is a non-equilibrium steady-state value, resulting from the enhanced abundance of CH and O predicted by our kinetics model. The impact of this reaction has not been fully explored and is outside the scope of this paper. In the absence of any significant ionizing source, if either chemical quenching or photodissociation enhance the abundances of O and CH significantly, the degree of ionization would then be enhanced, and ion–neutral chemistry may become important even in these regions.

Ammonia

In the case of ammonia, we do not invoke quenching at all. The species NH has a reasonable thermochemical volume fraction in the upper atmosphere (Bilger *et al.* 2013). Ammonia has a straight-forward connection to the cosmic-ray ionization rate via the reactions:



As such, its volume fraction follows the cosmic-ray flux somewhat closely, at least in the upper atmosphere; for higher pressures nitrogen becomes locked into N_2 . Our model predicts an abundance of NH_3 in the upper atmospheres almost five orders of magnitude enhanced, bringing the volume fraction from $\sim 10^{-12}$ to $\sim 10^{-7}$. Our model therefore predicts observable quantities of ammonia in the upper atmospheres of free-floating giant gas planets, in regions where the cosmic rays are not effectively shielded by the magnetic field. As such, for low-mass substellar objects, this may conceivably be a source of variability.

Conclusions

The application of Rimmer & Helling (2013) to a model atmosphere calculated using DRIFT-PHOENIX with $\log g = 3$ and $T_{\text{eff}} = 1000 \text{ K}$ provides us with an ionization rate. We include the ionization rate, as well as the temperature profile, atmospheric number density and elemental abundances as input parameters to a time-dependent chemical network. This allows us to calculate the number density of ions as well as the abundances of a variety of atomic and molecular species.

The ion–neutral chemistry is responsible for much of the prebiotic chemistry. This preliminary approach to exoplanet ion–neutral chemistry suggests that it is significant for producing hydrocarbon chains, and may help to drive PAH production in oxygen-rich atmospheres, possibly giving the upper atmospheres of these planets a chemistry similar to that expected from those objects with an enhanced C/O ratio. Finally, chemi-ionization processes may also significantly enhance the electron fraction in the cloud layer, if the abundances of atomic oxygen and CH are both above their equilibrium values. The formation of saturated carbon chains is closely connected to the formation of amino acids and other important pre-biotic species. Our results suggest that ion–neutral chemistry has a role to play in hydrogen-dominated environments at altitudes of $\sim 1 \mu\text{bar}$, and seems, at least without fast mixing and UV photochemistry present in atmospheres of irradiated planets, to generally enhance the abundances of some complex hydrocarbons, some of which may be relevant to prebiotic chemistry.

This work on a free-floating exoplanet may also be applicable to the directly imaged exoplanets orbiting HR 8799, but in order to explore this mechanism for the haze in the upper atmosphere of the exoplanet HD 189733 b we need to model the atmospheric chemistry for an irradiated exoplanet. It will then be important to account for the effect of the magnetic field of the host star as well as the planet upon cosmic-ray transport. The effect of stellar winds and their interaction with the magnetic field of the giant gas planet may also become important (see, e.g., Vidotto *et al.* 2012). It will also be necessary for ion–neutral chemical models to provide absolute abundances instead of ratios. Although the result of this work has indicated significant trends, and suggests that ion–neutral chemistry may be important part of the

atmospheric chemistry of free-floating giant gas planets, much work still needs to be done to develop a useful ion–neutral gas-phase network appropriate for the atmospheres of giant gas planets, both free-floating and the hot Jupiters.

Acknowledgements

We highlight financial support of the European Community under the FP7 by an ERC starting grant. We thank Peter Woitke for his help with determining timescales to chemical equilibrium. We also thank the anonymous referees for comments that have significantly improved the quality of this paper. This research has made use of NASA's Astrophysics Data System. We thank Ian Taylor for his technical support.

References

- Aikawa, Y., Umembayashi, T., Nakano, T. & Miyama, S.M. (1999). Evolution of molecular abundances in proto-planetary disks with accretion flow. *Astrophys. J.* **519**(2), 705.
- Bean, J.L., Miller-Ricci Kempton, E. & Homeier, D. (2010). A ground-based transmission spectrum of the super-Earth exoplanet GJ 1214b. *Nature* **468**, 669–672.
- Bilger, C., Rimmer, P. & Helling, C. (2013). Small hydrocarbon molecules in cloud-forming brown dwarf and giant gas planet atmospheres. *Mon. Not. R. Astron. Soc.* **435**, 1888–1903.
- Borucki, W.J., Levin, Z., Whitten, R.C., Keesee, R.G., Capone, L.A., Summers, A.L., Toon, O.B. & Dubach, J. (1987). Predictions of the electrical conductivity and charging of the aerosols in Titan's atmosphere. *Icarus* **72**, 604–622.
- Capone, L.A., Dubach, J., Whitten, R.C., Prasad, S.S. & Santhanam, K. (1980). Cosmic ray synthesis of organic molecules in Titan's atmosphere. *Icarus* **44**, 72–84.
- Capone, L.A., Dubach, J., Prasad, S.S. & Whitten, R.C. (1983). Galactic cosmic rays and N₂ dissociation on Titan. *Icarus* **55**, 73–82.
- Dehn, M. (2007). *PhD Thesis*, University of Hamburg.
- Demory, B.-O. et al. (2011). The high Albedo of the hot Jupiter Kepler-7 b. *Astrophys. J.* **735**, L12.
- Frenklach, M. & Feigelson, E.D. (1989). Formation of polycyclic aromatic hydrocarbons in circumstellar envelopes. *Astrophys. J.* **341**, 372–384.
- Gredel, R., Lepp, S., Dalgarno, A. & Herbst, E. (1989). Cosmic-ray-induced photodissociation and photoionization rates of interstellar molecules. *Astrophys. J.* **347**, 289–293.
- Gurnett, D.A., Shaw, R.R., Anderson, R.R. & Kurth, W.S. (1979). Whistlers observed by Voyager 1 – detection of lightning on Jupiter. *Geophys. Res. Lett.* **6**, 511–514.
- Harada, N., Herbst, E. & Wakelam, V. (2010). A new network for higher-temperature gas-phase chemistry. I. A preliminary study of accretion disks in active galactic nuclei. *Astrophys. J.* **721**, 1570–1578.
- Helling, C. et al. (2008). A comparison of chemistry and dust cloud formation in ultracool dwarf model atmospheres. *Mon. Not. R. Astron. Soc.* **391**, 1854–1873.
- Helling, C., Jardine, M. & Mokler, F. (2011). Ionization in atmospheres of brown dwarfs and extrasolar planets. II. Dust-induced collisional ionization. *Astrophys. J.* **737**, 38.
- Hoyle, F. & Wickramasinghe, N.C. (2000). *Astronomical Origins of Life: Steps towards Panspermia*. Kluwer Academic Publishers, Dordrecht.
- Krestinin, A.V. (2000). Detailed modeling of soot formation in hydrocarbon pyrolysis. *Combust. Flame* **121**(3), 513.
- Lavvas, P., Yelle, R.V. & Vuitton, V. (2009). The detached haze layer in Titan's mesosphere. *Icarus* **201**, 626–633.
- Liang, M.-C., Yung, Y.L. & Shemansky, D.E. (2007). Photolytically generated aerosols in the mesosphere and thermosphere of Titan. *Astrophys. J.* **661**, L199–L202.
- Lodders, K. (2004). Jupiter formed with more tar than ice. *Astrophys. J.* **611**, 587–597.
- MacGregor, M. & Berry, R.S. (1973). Formation of HCO⁺ by the associative ionization of CH + O. *J. Phys. B At. Mol. Phys.* **6**, 181–196.
- McElroy, D., Walsh, C., Markwick, A.J., Cordiner, M.A., Smith, K. & Millar, T.J. (2013). The UMIST database for astrochemistry 2012. *Astron. Astrophys.* **550**, A36.
- Millar, T.J., Farquhar, P.R.A. & Willacy, K. (1997). The UMIST database for astrochemistry 1995. *Astron. Astrophys. Suppl.* **121**, 139–185.
- Miller, S.L. & Cleaves, H.J. (2006). Prebiotic chemistry on the primitive earth. *Syst. Biol.: Vol. I: Genom.: Vol. I: Genom.* **1**, 1.
- Molina-Cuberos, G.J., López-Moreno, J.J., Rodrigo, R. & Lara, L.M. (1999a). Chemistry of the galactic cosmic ray induced ionosphere of Titan. *J. Geophys. Res.* **104**, 21997–22024.
- Molina-Cuberos, G.J., López-Moreno, J.J., Rodrigo, R., Lara, L.M. & O'Brien, K. (1999b). Ionization by cosmic rays of the atmosphere of Titan. *Planet. Space Sci.* **47**(10–11), 1347.
- Moses, J.I., Bézard, B., Lellouch, E., Gladstone, G.R., Feuchtgruber, H. & Allen, M. (2000). Photochemistry of Saturn's atmosphere. I. Hydrocarbon chemistry and comparisons with ISO observations. *Icarus* **143**, 244–298.
- Moses, J.I., Fouchet, T., Bézard, B., Gladstone, G.R., Lellouch, E. & Feuchtgruber, H. (2005). Photochemistry and diffusion in Jupiter's stratosphere: constraints from ISO observations and comparisons with other giant planets. *J. Geophys. Res. (Planets)* **110**, 8001.
- Moses, J.I. et al. (2011). Disequilibrium carbon, oxygen, and nitrogen chemistry in the atmospheres of HD 189733b and HD 209458b. *Astrophys. J.* **737**, 15.
- Orgel, L.E. (1998). The origin of life – a review of facts and speculations. *Trends Biochem. Sci.* **23**(12), 491–495.
- Pont, F., Knutson, H., Gilliland, R.L., Moutou, C. & Charbonneau, D. (2008). Detection of atmospheric haze on an extrasolar planet: the 0.55–1.05 μm transmission spectrum of HD 189733b with the HubbleSpaceTelescope. *Mon. Not. R. Astron. Soc.* **385**, 109–118.
- Porco, C.C. et al. (2005). Imaging of Titan from the Cassini spacecraft. *Nature* **434**, 159–168.
- Prasad, S.S. & Tarafdar, S.P. (1983). UV radiation field inside dense clouds – its possible existence and chemical implications. *Astrophys. J.* **267**, 603–609.
- Rages, K. & Pollack, J.B. (1983). Vertical distribution of scattering hazes in Titan's upper atmosphere. *Icarus* **55**, 50–62.
- Rimmer, P. & Helling, C. (2013). Ionization in atmospheres of Brown Dwarfs and extrasolar planets IV. The Effect of Cosmic Rays. *ArXiv e-prints*.
- Rimmer, P.B., Herbst, E., Morata, O. & Roueff, E. (2012). Observing a column-dependent ζ in dense interstellar sources: the case of the Horsehead nebula. *A&A* **537**, A7.
- Showman, A.P., Fortney, J.J., Lian, Y., Marley, M.S., Freedman, R.S., Knutson, H.A. & Charbonneau, D. (2009). Atmospheric circulation of hot Jupiters: coupled radiative-dynamical general circulation model simulations of HD 189733b and HD 209458b. *Astrophys. J.* **699**, 564–584.
- Shull, J.M. & Hollenbach, D.J. (1978). H₂ cooling, dissociation, and infrared emission in shocked molecular clouds. *Astrophys. J.* **220**, 525–537.
- Shumilov, O.I., Kasatkina, E.A., Henriksen, K. & Vashenyuk, E.V. (1996). Enhancement of stratospheric aerosols after solar proton event. *Ann. Geophys.* **14**, 1119–1123.
- Sing, D.K. et al. (2011). Hubble Space Telescope transmission spectroscopy of the exoplanet HD 189733b: high-altitude atmospheric haze in the optical and near-ultraviolet with STIS. *Mon. Not. R. Astron. Soc.* **416**, 1443–1455.
- Sittler, E.C., Hartle, R.E., Bertucci, C., Coates, A., Cravens, T., Dandouras, I. & Shemansky, D. (2010). *Energy Deposition Processes in Titan's Upper Atmosphere and Its Induced Magnetosphere*, p. 393.
- Skilling, J. & Strong, A.W. (1976). Cosmic ray exclusion from dense molecular clouds. *Astron. Astrophys.* **53**, 253–258.
- Stark, C.R., Helling, C., Diver, D.A. & Rimmer, P.B. (2013). *ApJ* **776**, 11.
- Velinov, P.I.Y. & Mateev, L.N. (2008). Improved cosmic ray ionization model for the system ionosphere atmosphere – calculation of electron production rate profiles. *J. Atmos. Sol.-Terres. Phys.* **70**, 574–582.

- Velinov, P.I.Y., Mishev, A. & Mateev, L. (2009). Model for induced ionization by galactic cosmic rays in the Earth atmosphere and ionosphere. *Adv. Space Res.* **44**, 1002–1007.
- Venot, O., Hébrard, E., Agúndez, M., Dobrijevic, M., Selsis, F., Hersant, F., Iro, N. & Bounaceur, R. (2012). A chemical model for the atmosphere of hot Jupiters. *ArXiv e-prints*.
- Vidotto, A.A., Fares, R., Jardine, M., Donati, J.-F., Opher, M., Moutou, C., Catala, C. & Gombosi, T.I. (2012). The stellar wind cycles and planetary radio emission of the τ Boo system. *Mon. Not. R. Astron. Soc.* **423**, 3285–3298.
- Visscher, C. & Moses, J.I. (2011). Quenching of carbon monoxide and methane in the atmospheres of cool brown dwarfs and hot Jupiters. *Astrophys. J.* **738**(1), 72.
- Wakelam, V., Selsis, F., Herbst, E. & Caselli, P. (2005). Estimation and reduction of the uncertainties in chemical models: application to hot core chemistry. *Astron. Astrophys.* **444**, 883–891.
- Wakelam, V. *et al.* (2012). A KInetic Database for astrochemistry (KIDA). *Astrophys. J. Suppl.* **199**, 21.
- Whitten, R.C., Borucki, W.J., O'Brien, K. & Tripathi, S.N. (2008). Predictions of the electrical conductivity and charging of the cloud particles in Jupiter's atmosphere. *J. Geophys. Res. (Planets)* **113**, 4001.
- Wilson, E.H. & Atreya, S.K. (2003). Chemical sources of haze formation in Titan's atmosphere. *Planet. Space Sci.* **51**, 1017–1033.
- Witte, S., Helling, C. & Hauschildt, P.H. (2009). Dust in brown dwarfs and extra-solar planets. II. Cloud formation for cosmologically evolving abundances. *Astron. Astrophys.* **506**, 1367–1380.
- Woitke, P. & Helling, C. (2004). Dust in brown dwarfs. III. Formation and structure of quasi-static cloud layers. *Astron. Astrophys.* **414**, 335–350.
- Woitke, P., Kamp, I. & Thi, W.-F. (2009). Radiation thermo-chemical models of protoplanetary disks. I. Hydrostatic disk structure and inner rim. *Astron. Astrophys.* **501**, 383–406.
- Woods, P.M. & Willacy, K. (2007). Benzene formation in the inner regions of protostellar disks. *Astrophys. J. Lett.* **655**(1), L49.
- Zahnle, K., Marley, M.S., Freedman, R.S., Lodders, K. & Fortney, J.J. (2009). Atmospheric sulfur photochemistry on hot Jupiters. *Astrophys. J.* **701**, L20–L24.